Nat Neurosci. Author manuscript; available in PMC 2014 June 26.

Published in final edited form as:

Nat Neurosci. 2013 March ; 16(3): 300–308. doi:10.1038/nn.3321.

Insulin induces long-term depression of VTA dopamine neurons via an endocannabinoid-mediated mechanism

Gwenaël Labouèbe[1,4,*], **Shuai Liu**[1,5,*], **Carine Dias**[2], **Haiyan Zou**[1], **Jovi C.Y. Wong**[1], **Subashini Karunakaran**[3], **Susanne M. Clee**[3], **Anthony Phillips**[2], **Benjamin Boutrel**[4], and **Stephanie L. Borgland**[1,5]

[1]Department of Anesthesiology, Pharmacology and Therapeutics, The University of British Columbia, 212-2176 Health Sciences Mall, Vancouver, BC, V6T 1Z3, CANADA [2]Department of Psychiatry, The University of British Columbia, 2255 Health Sciences Mall, Vancouver, BC, V6T 2A1, CANADA [3]Department of Cellular and Physiological Sciences, The University of British Columbia, Life Sciences Centre, 2350 Health Sciences Mall, Vancouver, BC, V6T 1Z3, CANADA [4]Center for Psychiatric Neuroscience, Department of Psychiatry, Site de Cery, 1008 Prilly, Lausanne University Hospital, Switzerland [5]State Key Laboratory of Medical Neurobiology, Shanghai Medical College, Fudan University, China

Abstract

The prevalence of obesity has drastically increased over the last few decades. Exploration into how hunger and satiety signals influence the reward system can help us to understand non-homeostatic mechanisms of feeding. Evidence suggests that insulin may act in the ventral tegmental area (VTA), a critical site for reward-seeking behavior, to suppress feeding. However, the neural mechanisms underlying insulin effects in the VTA remain unknown. We demonstrate that insulin, a circulating catabolic peptide that inhibits feeding, can induce a long-term depression (LTD) of excitatory synapses onto VTA dopamine neurons. This effect requires endocannabinoid-mediated presynaptic inhibition of glutamate release. Furthermore, after a sweetened high fat meal, which elevates endogenous insulin levels, insulin-induced LTD is occluded. Finally, insulin in the VTA reduces food anticipatory behavior and conditioned place preference for food. Taken together, these results suggest that insulin in the VTA suppresses excitatory synaptic transmission and reduces salience of food-related cues.

Keywords

Insulin; Ventral Tegmental Area; Dopamine; LTD; AMPA receptors; obesity; CB1 receptor; endocannabinoid; conditioned place preference; incentive salience

[6]To whom correspondence should be addressed: Borgland@mail.ubc.ca, Tel: +1 604 822 7826, Fax: +1 604 822 6012.
[*]These authors contributed equally to this study

Obesity is now recognized as a serious public health issue because of its increasing prevalence and serious comorbidities, including type 2 diabetes, cancer and cardiovascular diseases [1]. Obesity results from increased energy consumption that exceeds energy expenditure. While much research has focused on central nervous system regulation of body weight homeostasis and metabolism, this system does not work very well in an environment where little effort is required to procure palatable food with high caloric density. Dopamine neurons of the ventral tegmental area (VTA) have been implicated in the incentive, reinforcing, and motivational aspects of food intake [2]. Synapses onto VTA dopamine neurons can undergo both long-term potentiation (LTP) and long-term depression (LTD) to regulate their synaptic strength and consequent dopaminergic output [3, 4]. Enhanced synaptic efficacy of these neurons has been linked not only to exposure to drugs of abuse, but to feeding-related peptides, such as hypocretin/orexin [5, 6] and ghrelin [7]. Potentiation of synaptic strength of dopamine neurons by feeding-promoting peptides may underlie motivation to obtain food [5, 8, 9].

Normal feeding is regulated by the circulating catabolic peptides, insulin and leptin, that transmit satiety signals to the brain. Insulin is released into the circulation after ingestion of a meal and, along with leptin, may signal the cessation of eating by action in the ventromedial hypothalamus in response to changes in energy homeostasis [10]. Insulin gains access to the brain by active transport across the blood-brain barrier [11] and its effects are mediated by signaling through insulin receptors expressed throughout the brain [12]. Insulin binds to a single-pass tyrosine kinase membrane receptor, resulting in dimerization and activation of its intrinsic kinase domain. Insulin-response substrates are phosphorylated, and then mediate intracellular signaling cascades and transcription. Obesity often results in resistance to insulin signaling and consequently circulating levels of both glucose and insulin remain high [1]. Obesity-associated hyperinsulinemia leading to insulin resistance has also been reported in the brain [1, 13].

While leptin can inhibit firing of dopamine neurons and reduce dopaminergic output [14, 15], little is known about how insulin interacts with dopamine neurons within the VTA. Several lines of evidence suggest that insulin may alter activity of VTA dopamine neurons. Insulin receptors are expressed on dopamine neurons [16]. When administered intracerebroventricularly, insulin decreases motivation to obtain sucrose [17] and inhibits conditioned place preference (CPP) associated with high fat food [18]. Insulin administered directly into the VTA inhibits opioid-induced feeding [19] and palatable food ingestion [20,21]. Furthermore, insulin in the VTA increases threshold for intracranial self-stimulation[22]. Therefore, although insulin appears to modulate appetitive behavior, it is unknown how insulin modulates excitatory synaptic transmission of dopamine neurons. Modulation of excitatory inputs onto VTA dopamine neurons is particularly important as these inputs tightly regulate dopamine neuronal firing and ultimately dopamine release[23]. To elucidate the potential contributions of insulin signaling to neuroplasticity in the VTA, we explored the effects of insulin on excitatory synaptic transmission onto VTA dopamine neurons.

Results

Insulin depresses AMPAR-mediated synaptic transmission of VTA dopamine neurons

The VTA receives glutamatergic inputs from a variety of regions including the lateral hypothalamus, prefrontal cortex, lateral dorsal tegmentum and peduncle pontine nucleus[24]. Excitatory postsynaptic currents (EPSCs) from unspecified glutamatergic inputs were evoked using a bipolar stimulating electrode placed 100 – 300 μm rostral to the recording electrode on VTA dopamine neurons recorded from mouse horizontal midbrain slices. Bath application of insulin (500 nM, 10 min; [25, 26]) induced a long-term depression (LTD) of evoked EPSCs amplitude (Figure 1A). To determine if insulin-induced LTD required insulin receptor signaling, we interfered with insulin receptor activation in two ways. Both intracellular application of a tyrosine kinase inhibitor, HNMPA (300 μM; [27]), or bath application of a novel insulin receptor antagonist, S961 (1 μM; [28]), blocked insulin-induced LTD (Figure 1A). Because insulin is also known to target insulin-like growth factor receptors (IGFR) in the brain [29], we blocked IGFR activation using the selective inhibitor picropodophyllotoxin (PPP; 0.5 μM). In the presence of PPP, insulin-induced LTD was not significantly different from the control condition ($p > 0.05$, T-test comparing maximal effects at 40 min of PPP-treated vs. control), therefore demonstrating the specificity of insulin action via insulin receptors. Insulin-induced LTD was concentration-dependent with an IC_{50} of 17 ± 1 nM (Figure 1B). Finally, to determine if insulin-induced LTD was due to ineffective insulin wash out from midbrain slices, we bath applied cell permeable $HNMPA[AM]_3$ (1 μM; Figure 1C) or S961 (300 μM; Figure 1D) 10 min after washout of insulin. Insulin-induced LTD was not reversed by either the insulin receptor antagonist or insulin receptor tyrosine kinase inhibitor.

To determine if insulin could alter NMDAR-mediated excitatory synaptic transmission, we evoked NMDAR EPSCs while voltage-clamping dopamine neurons at +40 mV. Insulin (500 nM, 10 min) caused a long lasting depression of NMDAR EPSCs to a maximum of 36 ± 5 % (Figure 1E). The time course or maximal effect was not significantly different than that for insulin-induced LTD of AMPAR EPSCs ($p > 0.05$; T-test comparing areas under the curve (AUC)). Taken together, insulin suppressed both AMPAR and NMDAR EPSCs of VTA dopamine neurons.

While insulin depressed excitatory synaptic transmission of VTA dopamine neurons, we investigated if insulin could also affect inhibitory synaptic transmission onto these neurons. Insulin did not modify $GABA_A$ mediated inhibitory postsynaptic currents (IPSCs) onto dopamine neurons (Figure 1F; $p > 0.05$, T-test comparing maximal effect at 40 min to control (Figure 1A)), suggesting that insulin-induced LTD occured selectively at excitatory synapses.

Insulin-induced LTD requires the activation of Akt and mTOR

Insulin receptor activation triggers a variety of signal transduction cascades upon dimerization, autophosphorylation, and recruitment of insulin receptor substrates. One pathway involves activation of phosphatidylinositol 3 kinase (PI3K) and subsequent stimulation of Akt kinase. This pathway also triggers activation of mammalian target of

rapamycin (mTOR) [30], a mediator that has been implicated in depression of AMPAR-mediated synaptic transmission of VTA dopamine neurons [31]. To determine if mTOR signaling was required for insulin-induced LTD in the VTA, we prevented activation of mTOR by bath application of rapamycin (50 nM). Rapamycin significantly blocked insulin-induced LTD (Figure 2A, B) compared to controls (Figure 1A, $p < 0.05$, T-test of maximal effects at 40 min). Insulin-induced LTD was also abolished in the presence of the intracellularly applied Akt antagonist, 10-DEBC (20 μM; Figure 2A, B , $p > 0.05$, paired T-test of maximal effect at 40 min to baseline at 5 min) and was significantly different from insulin-induced LTD in controls (Figure 1A, $p < 0.05$, T-test of maximal effects at 40 min). In contrast, insulin-induced LTD was unaffected in the presence of the protein kinase A inhibitor, PKI (20 μM; Figure 2A, B; $p > 0.05$, T-test of maximal effects at 40 min). Figure 2B summarizes the maximal effect 20 min after insulin application. A one-way ANOVA with a Dunnet's post hoc test comparing treatments to the control demonstrated that the effect of insulin in 10-DEBC or rapamycin was significantly different than insulin alone ($p < 0.01$, $p < 0.05$, respectively). These data suggest that the Akt/mTOR pathway was required for insulin-induced LTD in VTA dopaminergic neurons.

Insulin-induced LTD of AMPARs is not mediated by AMPAR trafficking

Insulin-induced LTD in hippocampal and cerebellar neurons involves internalization of AMPARs [25, 26]. Therefore, we tested whether insulin-induced LTD in the VTA occurred via activity-dependent internalization. This process requires AMPAR sequestration through a clathrin-dependent mechanism, association with dynamin and amphiphysin, and consequent dephosphorylation of components of the endocytotic machinery[32]. We applied $GluA2_{3Y}$ (100 μg/ml; [33]; Figure 3A) or Δpep849-853 (500 μM; [34]; Figure 3B) intracellularly to block the AP2 binding site on the AMPA GluA2 receptor subunit. Maximal inhibition was not significantly different from controls ($GluA2_{3Y}$: 31 ± 8%, $p > 0.05$; Δpep849-853: 34 ± 4%, $p > 0.05$; T-test comparing effect at 40 min of $GluA2_{3Y}$ or Δpep849-853 treated neurons to controls from Figure 1A). Furthermore, intracellular application of D15, a peptide which disrupts the interaction between dynamin and amphiphysin [35], did not significantly alter the magnitude of insulin-induced LTD in VTA dopamine neurons (37 ± 9% decrease 30 min after insulin application; Figure 3C, D; $p > 0.05$; T-test comparing maximal effect at 40 min in D15-treated cells with that of controls). LTD of synapses of dopamine neurons in the VTA can also be induced by low-frequency stimulation of glutamatergic afferents (LFS-LTD; Figure 3E, F; [3]). Intracellular application of D15, but not the scrambled peptide S15, abolished LFS-LTD compared to controls in VTA dopamine neurons (Figure 3E, F; $p < 0.05$; ANOVA of maximal effect at 40 min of LFS-LTD in D15- or S15-treated cells to LFS-LTD in untreated controls). Taken together, these results suggest that while D15 blocked conventional LFS-LTD in the VTA, insulin-induced LTD occured by some other mechanism.

Insulin decreases presynaptic glutamate release onto VTA dopamine neurons via retrograde endocannabinoid signaling

LTD in the VTA can be mediated postsynaptically as described above, or by a presynaptic inhibition of glutamate release [36]. Therefore, to investigate whether insulin altered the number and/or function of postsynaptic AMPARs or caused a presynaptic inhibition of glutamate release, we measured AMPAR-mediated miniature EPSCs (mEPSCs), a standard

method for determining the locus of synaptic change[37]. 20 min after bath application of insulin (500 nM, 10 min), mEPSCs frequency was significantly reduced compared to untreated slices (ACSF, 10 min) (Figure 4A, Bi, Ci; $p < 0.01$; T-test comparing frequency of mEPSCs from ACSF- vs. insulin-treated cells). Insulin did not alter mEPSCs amplitude compared to untreated slices (Figure 4A, Bii, Cii; $p > 0.05$; T-test comparing amplitude of mEPSCs from ACSF- vs. insulin-treated cells). A reduction of mEPSCs frequency concomitant with unchanged amplitude likely reflects a decrease in the probability of presynaptic neurotransmitter release [37]. To further verify if insulin-mediated depression of AMPARs was mediated pre- or post-synaptically, we examined the effects of insulin on the probability of transmitter release, comparing the response to paired pulses, a measure that changes in a highly predictable fashion with release probability. We recorded AMPAR EPSCs at −70 mV using a paired-pulse stimulation protocol with a 50-ms interval and observed significant paired pulse facilitation after insulin bath application (Figure 4D; $p < 0.05$, repeated measures ANOVA). Thus, insulin-mediated depression of AMPAR-mediated synaptic transmission resulted from a reduced probability of glutamate release.

Interestingly, antagonists of the insulin receptor signaling pathway administered postsynaptically was sufficient to block insulin-mediated LTD, yet insulin caused a presynaptic depression of glutamate release. Therefore, we hypothesized that postsynaptic insulin-receptor activation may initiate a retrograde signaling mechanism. Endocannabinoids synthesized postsynaptically act at presynaptic cannabinoid 1 receptors (CB1Rs) in a retrograde manner to mediate presynaptic inhibition of glutamate release in several brain regions including the VTA [38, 39]. Therefore, we tested if the insulin-induced inhibition of glutamate release probability was blocked in the presence of a CB1R antagonist, AM251 (2 μM, bath applied 5 min prior to insulin and for the duration of the experiment). Insulin did not significantly alter mEPSCs frequency (Figure 4E, Fi, Gi; $p > 0.05$; T-test comparing frequency of mEPSCs from ACSF vs. insulin treated cells) or amplitude (Figure 4E, Fii, Gii; $p > 0.05$; T-test comparing amplitude of mEPSCs from ACSF- vs. insulin-treated cells) in the presence of AM251.

To determine if CB1R activation was required for insulin-induced LTD, AM251 (2 μM) was bath applied 5 min prior to insulin (500 nM, 10 min) and for the duration of the experiment. Insulin-induced LTD was significantly reduced compared to controls (AM251 with insulin: 10 ± 7 % vs. insulin alone: 40 ± 3 % decrease 30 min after insulin application; Figure 5A; $p < 0.01$; T-test). Bath application of a CB1R agonist, WIN 55,232-2 (WIN, 1 μM, 5 min), induced LTD of AMPAR-mediated synaptic transmission with a similar magnitude as insulin-mediated LTD (44 ± 4% decrease 35 min after WIN application; Supplemental Figure 1; $p > 0.05$; T-test). To determine if prior activation of CB1Rs could occlude insulin-induced LTD, we applied WIN 20 min prior to insulin and for the duration of the experiment. In the presence of WIN, insulin did not induce a significant depression of AMPAR-mediated synaptic transmission (Figure 5B; $p > 0.05$; paired T-test of baseline (5 min) vs. 30 min after insulin application), suggesting that insulin-induced LTD and CB1R-mediated LTD shared the same mechanism. In the reverse experiment, we tested if WIN could further inhibit AMPAR EPSCs after insulin-induced LTD. WIN (1 μM, 5 min) applied 25 min after insulin application did not cause a significant reduction in evoked AMPAR EPSCs (Figure 5C; $p > 0.05$; paired T-test comparing effect at 40 min vs. 70 min).

We also examined if postsynaptic synthesis of endocannabinoids was required for insulin-induced LTD by inhibiting the synthesis of 2-arachidonylglycerol (2-AG), the most abundant endocannabinoid in the midbrain [40]. Intracellular application of the diacylglycerol lipase (DAGL) inhibitor, orlistat (2 μM), blocked insulin-induced LTD (Figure 5D; $p > 0.05$; paired T-test of baseline (5 min) compared to 30 min after insulin application). When compared to insulin treatment alone, preincubation of AM251, WIN or intracellular application of orlistat significantly inhibited insulin-induced LTD of AMPAR EPSCs ($p < 0.05$; ANOVA with Dunnet's post hoc test comparing treatments to insulin control). Taken together, these results suggest that insulin receptor activation stimulated 2-AG production resulting in presynaptic CB1R-mediated depression of glutamate release.

In other preparations, endocannabinoid-mediated LTD has been implicated in the induction phase of LTD, as depression of AMPAR EPSCs was resistant to CB1R antagonists several minutes after induction[39]. Therefore, we tested if insulin-induced LTD required CB1R activation or endocannabinoid synthesis solely during the LTD induction phase or if LTD was maintained by another mechanism. Application of AM251 (Figure 5E; $p > 0.05$) or orlistat (Figure 5E; $p > 0.05$) did not significantly alter AMPAR EPSC amplitude after insulin-induced LTD (T-tests comparing effect at 30 min vs. effect at 55 min). Taken together, our data suggest that endocannabinoids were required for induction of insulin LTD, but were no longer required to maintain the LTD.

To determine if intracellular calcium was required for insulin-induced LTD, the Ca^{2+} chelator BAPTA (10 mM) was applied intracellularly for the duration of the experiment. Insulin suppressed AMPAR EPSCs to a similar maximum as without BAPTA, suggesting that intracellular Ca^{2+} was not required for this effect (Figure 5F). Furthermore, insulin-induced LTD was still blocked by the CB1R antagonist, AM251, in the presence of intracellular BAPTA (Figure 5F), suggesting that intracellular Ca^{2+} was not required for insulin-induced endocannabinoid LTD.

Insulin-induced LTD in VTA is occluded after sweetened high-fat exposure

To determine if a caloric meal, known to elevate insulin levels, could alter insulin-induced LTD in the VTA, we exposed C57BL/6J mice to unlimited sweetened high-fat pellets (SHF group) or continued access to regular chow (RF group) for one hour before brain slice preparation. All mice were exposed to 1 g of SHF pellets 48 hours prior to the experiment to habituate them to the novel food. Plasma insulin levels were significantly greater in SHF group (2.0 ± 0.4 ng/ml, $n = 11$) compared to RF group (0.8 ± 0.2 ng/ml, $n = 7$) or 1 hour after SHF exposure (0.7 ± 0.2, $n = 9$) ($p < 0.05$; one way ANOVA). In contrast to dopamine neurons from RF fed animals ($n = 11$), insulin did not induce LTD in VTA dopamine neurons from SHF fed mice (Figure 6A, $n = 8$, $p > 0.05$; paired T-test comparing baseline at 5 min with 30 min after insulin application). The maximal effects of insulin on AMPAR EPSCs between RF- or SHF- fed mice were significantly different ($p < 0.05$, T-test). The inability of insulin to induce LTD could be explained by the possibility that SHF fed mice had elevated insulin levels, thus occluding the effects of exogenously applied insulin. To test this hypothesis, we measured mEPSCs from VTA dopamine neurons of mice fed RF or SHF. Compared to mice fed RF ($n = 8$), mice fed SHF had a significantly reduced mEPSC

frequency (Figure 6Bi,ii, iii, n = 10, $p < 0.05$, T-test), but no change in mEPSC amplitude compared to RF fed mice (Figure 6Bi,ii,iv, $p > 0.05$, T-test). We next tested if a SHF meal increased endocannabinoid signaling compared to controls. Bath application of the CB1R antagonist, AM251 (10 μM), led to a significant increase of AMPAR EPSC amplitude in VTA slices obtained from SHF fed animals (n = 6) compared to mice fed RF (n = 9) (Figure 6C; $p < 0.05$; T-test comparing maximal effect at 30 min between SHF and RF groups). To determine if continued endocannabinoid synthesis was required for the CB1R-mediated increase in EPSCs after SHF, orlistat was applied via the patch pipet before, during and after AM251 application (2 μM, Figure 6C). Intracellular application of orlistat did not significantly alter the maximal amplitude of AMPAR EPSCs after AM251 application to cells from SHF fed mice ($p > 0.05$, n = 9; T-test comparing AMPAR EPSCs 20 min after AM251 application with or without orlistat). To determine if 2-AG levels are produced by a source other than the postsynaptic neuron following SHF, we tested if bath application of orlistat altered AMPAR EPSCs after AM251 application to cells from mice fed SHF. In the presence of orlistat, AM251 did not alter AMPAR EPSCs in SHF fed mice ($p > 0.05$, n = 8, T-test comparing AMPAR EPSCS before (at 5 min) and after (at 30 min) AM251).

Next, we assessed if insulin-induced LTD was present in VTA dopamine neurons from mice fed SHF or RF (1 h) and then sacrificed 60 min after the food exposure. Insulin-induced LTD was partially restored in animals fed SHF (22 ± 7 % inhibition 30 min after insulin application; Figure 6D, E, $p < 0.05$, paired T-test comparing baseline at 5 min with maximum at 15 min after insulin application). Insulin-induced LTD was significantly different between dopamine neurons from RF fed animals, SHF fed animals and those from 1 hour after SHF fed animals (Figure 6D, E, $p < 0.05$, ANOVA with Bonferroni post-hoc test). Taken together, these results suggest that elevation of insulin levels by consumption of a caloric meal temporarily disrupts exogenously applied insulin-induced LTD in VTA slices.

To determine if a SHF meal could modulate a dopamine-mediated behavior, the effect of 1 hour access to SHF or RF on cocaine-induced locomotor activity was examined. As above, mice were given 1 hour access to SHF or RF. Mice were then given a systemic injection of cocaine (15 mg/kg, i.p.) or saline and then placed immediately in an open field chamber to measure locomotor activity (15 min). Mice given 1 hour access to SHF, exhibited significantly less locomotor activity than did mice fed with RF (Figure 6F, RF: 89 ± 8 cm vs. SHF: 73 ± 8 cm, $p < 0.05$, one way ANOVA). There were no significant differences in basal locomotor activity in mice receiving RF (37 ± 2 cm, n = 9) or SHF (34 ± 3 cm, n = 9, $p > 0.05$, one way ANOVA). These data suggest that a SHF meal can reduce cocaine-induced locomotor activity.

Insulin in the VTA inhibits food anticipatory activity, conditioned place preference (CPP) for food, but not effort to obtain food reward

To explore the behavioral relevance of insulin in the VTA, we first assessed if insulin could modulate food anticipatory activity. Previous work has demonstrated that mice will increase their locomotor activity prior to receiving meals[41], an effect that is accompanied by a significant increase in dopamine concentration in target regions of the VTA[42]. Mice were entrained to consume their daily caloric intake within 4 hours per day between ZT 6–10.

Once entrainment was established, on the test day mice received VTA injections of insulin (5 mU; [20]) or vehicle and then placed in the entrainment cage in which food was placed behind a plexiglass barrier containing 4 small diameter holes at the base of the barrier. In this paradigm, mice had visual and olfactory cues of the food (chow), but were unable to access the food for 15 minutes. During this time, food anticipatory activities including cage crossovers as a proxy for locomotor activity, rearing and digging were recorded. Non-specific behavioral activities such as grooming were also recorded. Intra-VTA insulin significantly reduced crossovers (Figure 7Ai, $p < 0.05$, paired T-test), rearing (Figure 7Aii, $p < 0.05$, paired T-test) and digging ($p < 0.05$, paired T-test, Figure 7Aiii), but did not reduce grooming (Figure 7Aiv, $p > 0.05$, paired T-test). Importantly, intra-VTA insulin (5 mU) did not modify basal locomotor activity in an open field (15 min) compared to intra-VTA vehicle (vehicle: 29 ± 4 cm vs. insulin: 31 ± 3, $n = 9$, $p > 0.05$, paired-T test). These data indicate that insulin in the VTA suppressed behavioral activities associated with food anticipatory behavior.

Insulin-induced reduction in activity during anticipation of food may reflect changes in simple appetitive behaviors displayed routinely prior to consumption of a meal; an effect that is mediated by the salience of food-related cues. Alternatively, insulin may reduce the effort exerted to obtain food. We first tested the latter idea directly by training mice to perform an instrumental response for palatable food under progressive ratio (PR) schedule whereby the response requirement to earn sucrose escalates after the delivery of each reinforcer. The maximal number of responses emitted to successfully complete the final ratio is defined as the breakpoint and is hypothesized to reflect the maximum effort an animal will exert to obtain a fixed amount of food[43]. Intra-VTA insulin (0.065 mU (2 μM;[44])) did not alter the breakpoint for sucrose (2.5%, 10 μl) compared to intra-VTA vehicle (Figure 7Bi, $p > 0.05$, paired T-test). To determine if intra-VTA insulin modulates the effort required to obtain a more salient reinforcer, mice were tested with sweetened condensed milk (SCM). While the breakpoint was significantly greater for SCM than sucrose ($p < 0.001$, T-test), the breakpoint for SCM was not significantly different between intra-VTA insulin (3.25 mU (100 μM)) and controls ($p > 0.05$, paired T-test). Furthermore, there were no significant differences in cumulative probability for sucrose (Figure 7Biii) or SCM (Figure 7Biv) between intra-VTA insulin ($p > 0.05$, Kolmogorov-Smirnov test). Taken together, these data indicate that insulin in the VTA does not alter the effort required to obtain a palatable reinforcer.

Next, we tested if insulin in the VTA can alter conditioned place preference (CPP) for food. This test depends on the animal learning to associate contextual cues with a food reward[45]. These experiments were performed in *ad libitum* fed animals during their light phase to be consistent with our electrophysiological experiments. Unfortunately, we were unable to obtain a reliable CPP in non-food restricted mice; therefore the experiment was repeated using rats as subjects. Consistent with our electrophysiological studies, insulin induced a similar LTD in rats to a maximum of 37 ± 3 % 30 min after insulin application ($n = 7$; Supplemental Figure 2). Rats were placed initially in a central compartment of the CPP chamber and had free access to separate compartments defined by specific visual and floor texture contextual cues paired with food (Froot loops) or no food (unpaired) on alternate days for 8 training days. There were no significant differences in place preference amongst

groups during the pre-test (Figure 7C, $p > 0.05$, ANOVA with a Bonferroni post test). On the test day (in the absence of Froot loops), insulin (0.005 mU (63 nM)[22] or 0.065 mU (2 μM)[44]) or vehicle was microinjected in the VTA 5 min prior to placing the animals in the CPP apparatus. Time spent in each chamber was recorded. Intra-VTA insulin caused a concentration-dependent decrease in preference score (Figure 7D, $p < 0.05$, ANOVA with a Bonferroni post test). Disruption in CPP supports the proposal that insulin in the VTA reduces the salience of contextual cues associated with food reward.

Discussion

The data presented here establish a novel mechanism for insulin function in the mesolimbic pathway. Insulin produced an LTD of AMPAR-mediated synaptic transmission onto VTA dopamine neurons. Importantly, insulin-induced LTD required postsynaptic activation of insulin receptor signaling, synthesis of endocannabinoids as well as presynaptic CB1R-mediated inhibition of glutamate release. Furthermore, insulin-induced LTD was likely occluded in mice pre-fed with SHF. Insulin in the VTA inhibited food anticipatory behavior and CPP for food, suggesting that insulin may attenuate the salience of food-related contexts or cues. These data not only point to a novel type of endocannabinoid-mediated LTD, they demonstrate that insulin signaling in the VTA depresses synaptic output and plays a role in modulating ingestive behavior.

Insulin-induced LTD of VTA dopamine neurons

We demonstrated that insulin caused a long-lasting depression of AMPAR-mediated excitatory synaptic transmission onto VTA dopaminergic neurons with concentrations as low as 10 nM. Insulin-induced LTD has been reported in other brain regions, including the hippocampus [25] and cerebellum [26]. However, in these brain regions, insulin-induced LTD occurred through a clathrin-dependent endocytosis of GluA2-containing AMPARs. In contrast, we demonstrated that insulin-induced LTD was mediated by endocannabinoid retrograde signaling. First, insulin-induced LTD was not blocked by inhibitors to the endocytotic process of AMPARs. Secondly, insulin-induced LTD as well as insulin-induced reduction in mEPSCs frequency was abolished with AM251, a CB1R antagonist. Thirdly, we demonstrated that insulin- or CB1R-mediated depression of AMPAR currents occurred through the same mechanism. Fourth, intracellular application of orlistat, an inhibitor of 2-AG synthesis, blocked insulin-induced LTD. Taken together, we demonstrate a novel mechanism of insulin-induced LTD requiring retrograde endocannabinoid signaling.

Endocannabinoid-mediated LTD has been reported to occur at both excitatory [38] and inhibitory [46] synapses onto VTA neurons. Interestingly, insulin-induced endocannabinoid-mediated LTD was selective for glutamatergic synapses onto dopamine neurons as insulin receptor activation did not modify GABA IPSCs. While it is unclear how this synapse-selective endocannabinoid-LTD occurred, one possibility is that GABAergic and glutamatergic synapses are segregated within regions of the VTA, such that endocannabinoids produced near glutamatergic synapses may not reach GABAergic synapses. Interestingly, distal dendrites of dopamine neurons reaching into the substantia nigra reticulata received significantly stronger GABAergic input than dendrites nearer to the

substantia nigra pars compacta, thereby establishing precedence for synaptic segregation influencing neuronal activity within the midbrain [47]. Alternatively, insulin receptors could be preferentially located near glutamatergic synapses. Cell selective endocannabinoid-LTD has been demonstrated at excitatory synapses onto medium spiny neurons of the nucleus accumbens[48]. Taken together, insulin may selectively dampen glutamatergic inputs to the VTA.

Endocannabinoid-mediated LTD is a widespread phenomenon in the brain[39]. Its induction typically requires a transient increase in activity at glutamatergic afferents and concomitant release of endocannabinoids from the postsynaptic neuron. Endocannabinoid-mediated LTD can also result from activation of G-protein coupled receptors which signal through $G\alpha_{q/11}$, engaging phospholipase C (PLC) and DAGL, forming the endocannabinoid, 2-AG. Activation of $G\alpha_{i/o}$ -coupled receptors leading to increases in anandamide has also been demonstrated [39]. Here, we demonstrate a form of endocannabinoid-LTD that is initiated by activation of a receptor-tyrosine kinase-type receptor resulting in synthesis and release of 2-AG.

Although CB1 receptor activation is necessary for the induction of LTD, it is not necessary for its maintenance[39, 49, 50]. Consistent with these studies, we demonstrate that after exogenously applied insulin, LTD was not reversed with application of AM251 or orlistat. While application of WIN caused a long-lasting depression of AMPAR EPSCs, this was not likely due to persistent CB1R signaling, but the inability to wash out the highly lipophillic drug during the recording period[51]. These results implicate other mechanisms to maintain the LTD, including protein translation at excitatory synapses, as has been demonstrated in the striatum[51] or a presynaptic alteration stabilizing the reduced release probability.

Synaptic depression induced by SHF consumption

We demonstrated that synaptic depression onto dopamine neurons also occurs after a SHF meal. Although we are unable to unequivocally state that SHF induced synaptic depression was directly due to insulin signaling, this effect was consistent with insulin-induced LTD onto dopamine neurons. Firstly, when mice had 1 hour access to SHF plasma insulin levels were elevated compared to mice given RF. Secondly, compared to RF fed mice, SHF-fed mice demonstrated an inability to produce insulin-induced LTD and a decreased probability of glutamate release, suggesting that a SHF meal was sufficient to suppress excitatory synaptic transmission onto VTA dopamine neurons and potentially occlude insulin-induced LTD. Thirdly, only dopamine neurons from mice fed SHF were sensitive to a CB1R antagonist, suggesting an elevated endocannabinoid tone. Indeed, increased AEA and 2-AG levels were observed in animals fed a long-term high fat diet[52]. Bath application of orlistat inhibited the AM251-induced potentiation of AMPAR EPSCs after SHF. Interestingly, postsynaptic application of orlistat did not block AM251-induced potentiation of AMPAR EPSCs; however, there are several interpretations of this data. Firstly, intracellular application of orlistat would only block 2-AG production from the recorded neuron without negating potential increases in 2-AG due to insulin signaling on other dopamine neurons, or sources other than dopamine neurons contributing to the elevated endocannabinoid tone. Secondly, consistent with our *in vitro* results where exogenous application of insulin did not

require prolonged endocannabinoid release, 2-AG produced during the induction phase (during SHF consumption) was sufficient to maintain CB1R activation. Taken together, SHF meal induced a suppression of excitatory synaptic transmission onto dopaminergic neurons, likely by increasing endocannabinoid tone.

Interestingly, SHF-induced depression of excitatory synaptic transmission in the VTA was partially reversed in slices cut 1 hour after SHF food exposure. Thus, unlike long-lasting synaptic adaptations associated with drugs of abuse[53], the depression of excitatory synaptic transmission onto dopamine neurons associated with a caloric meal was relatively transient. Notably, one hour later, plasma insulin levels were significantly less than immediately after SHF, suggesting that the inability of exogenously applied insulin to induce LTD after SHF correlates with plasma insulin levels. Because of insulin's rapid clearance from the circulation by the liver, insulin has a very short half life *in vivo*[54]. Consequently, concentrations acting in the VTA may be different than that of exogenously applied insulin resulting in potential differences in the time course of effect. Additionally, *in vivo* mechanisms may be required to reverse SHF-induced synaptic depression. Indeed, arousal and feeding-related peptides such as orexin/hypocretin or ghrelin have been known to enhance excitatory synaptic efficacy onto VTA dopamine neurons[55–57]. Taken together, a depression of excitatory synaptic transmission onto dopamine neurons may transiently prevent depolarizations required for burst firing and delivery of dopamine to target regions of the VTA[58,59], thereby potentially attenuating the salience of food-related cues and consequent food consumption.

Interestingly, cocaine-induced locomotor activity was reduced in mice receiving a SHF meal compared to RF-fed controls. This effect is consistent with an increase in plasma insulin levels, an occlusion of insulin-induced LTD and a reduction of excitatory synaptic transmission onto VTA dopamine neurons after a SHF meal. Notably, this effect only occurred in cocaine-treated mice. Consistent with this, insulin in the VTA did not alter basal locomotor activity. Interestingly, insulin in the VTA increases transporter number or function resulting in a decrease in somatodendritic dopamine[60]. Therefore, in addition to a SHF meal reducing excitatory synaptic transmission, it may also reduce dopamine-enhanced locomotor activity.

Insulin in the VTA reduced salience of cues for food

Our electrophysiology results indicate that insulin suppressed excitatory synaptic transmission onto VTA dopamine neurons, likely reducing their burst activity which in turn would attenuate dopamine release in target regions of the mesocorticolimbic dopamine system. Enhanced synaptic efficacy onto VTA dopamine neurons and their consequent burst firing has been associated with learned associations of cues with rewards[59]. Therefore, we hypothesized that insulin in the VTA decreases salience of reward predicting cues. Consistent with this, we found decreased preference for environmental contexts associated with food after intra-VTA insulin treatment, in agreement with reports demonstrating i.c.v. insulin reduces CPP for high-fat food[18]. Surprisingly, we did not observe a significant effect on effort exerted to obtain sucrose or SCM with 0.065 or 3.25 mU insulin intra-VTA, respectively. While intra-VTA insulin (5 mU) did not modify lever pressing for sucrose

under a fixed ratio schedule[20], others have reported that icv insulin (5 mU), reduced lever pressing for 5% sucrose under a progressive ratio schedule[17]. Our observation that intra-VTA insulin suppressed food anticipatory behavior was likely an effect of insulin on processes involved in learned associations between visual and/or olfactory stimuli and food rather than those mediating effort required to obtain food *per se*. Importantly, unlike the PR test, consumption of food was not required for intra-VTA insulin-induced reductions of food anticipation or expression of food place preference. Consumption of RF was not reduced with intra-VTA insulin[60]. Furthermore, our study demonstrated that plasma insulin levels after RF feeding were not elevated, nor was exogenous insulin-induced LTD occluded after RF. However, a significant reduction in sated consumption of SHF was observed after intra-VTA insulin[60]. Therefore, intra-VTA insulin likely induced LTD and thus reduced salience for SHF resulting in reduced consumption. Taken together, insulin action in the VTA may reduce the salience of food-associated contexts or cues.

Here, we propose a novel mechanism by which insulin reduces excitatory synaptic efficacy onto VTA dopamine neurons. Insulin-induced LTD requires postsynaptic insulin receptor activation, Akt and mTOR signaling, and retrograde endocannabinoid suppression of glutamate release. Furthermore, a SHF meal, which elevates plasma insulin, transiently weakens excitatory synaptic transmission onto dopamine neurons. Finally, insulin in the VTA likely reduces the salience of cues or contexts associated with food. Taken together, these findings bring new insights to how insulin can modulate reward circuitry and a novel type of endocannabinoid-mediated LTD.

Methods

Animals

All protocols were in accordance with the ethical guidelines established by the Canadian Council for Animal care and were approved by the University of British Columbia Animal Care Committee. C57BL/6J mice were obtained from the University of British Columbia breeding facility. Mice expressing green fluorescent protein in neurons with tyrosine hydroxylase (TH-GFP mice) were obtained from Dr. Okano at the Keio University School of Medicine, Tokyo, Japan [61].

Electrophysiology

All electrophysiological recordings were performed in male mice ranging from P19 to P30. Briefly, animals were anesthetized with halothane, decapitated and brains were extracted. Horizontal sections of the VTA (250 μM) were prepared with a vibratome (Leica, Nussloch, Germany). Slices were placed in a holding chamber and allowed to recover for at least 1h before being placed in the recording chamber and superfused with bicarbonate-buffered solution (ACSF) saturated with 95% O_2/5% CO_2 and containing (in mM): 126 NaCl, 1.6 KCl, 1.1 NaH_2PO_4, 1.4 $MgCl_2$, 2.4 $CaCl_2$, 26 $NaHCO_3$, and 11 glucose (at 32°C–34°C). Cells were visualized using infrared differential interference contrast video microscopy. Whole-cell voltage-clamp recordings were made using a MultiClamp 700B amplifier (Axon Instruments, Union City, CA). Electrodes (3–4.5 MΩ) contained (in mM): 117 cesium methansulfonate, 20 HEPES, 0.4 EGTA, 2.8 NaCl, 5 TEA-Cl, 2.5 MgATP, and 0.25 NaGTP

(pH 7.2–7.3, 270–285 mOsm). Series resistance (10–25 MΩ) and input resistance were monitored online with a 10 mV depolarizing step (400 ms) given before every afferent stimulus. To identify VTA dopaminergic neurons, we recorded from TH-GFP mice which expressed GFP fluorescence in dopaminergic neurons. In C57BL/6J mice, dopamine neurons were identified by the presence of a hyperpolarizing cation current (I_h) [63, 64]. A bipolar stimulating electrode was placed 100–300 μm rostral to the recording electrode and was used to stimulate excitatory afferents at 0.1 Hz. To induce low-frequency stimulation LTD (LFS-LTD), neurons were held at −40 mV for 6 min while excitatory afferents were stimulated at 1 Hz. Neurons were voltage clamped at −60 mV to record AMPAR-mediated excitatory post synaptic currents (EPSCs) or $GABA_A$-mediated inhibitory post synaptic currents (IPSCs). NMDAR EPSCs were recorded while neurons were voltage clamped at +40 mV. EPSCs were recorded in the presence of picrotoxin (100 μM) in order to block $GABA_A$ receptor-mediated inhibitory postsynaptic currents (IPSCs) while DNQX (10 μM), Strychnine (1 μM) and DPCPX (1 μM) were added to isolate $GABA_A$ IPSCs. EPSCs and IPSCs were filtered at 2 kHz, digitized at 10 kHz, and collected online using pClamp 10 (Molecular Devices, Sunnyvale, CA). Currents traces were constructed by averaging 10 consecutive EPSCs/IPSCs. AMPAR miniature EPSCs (mEPSCs) were recorded in cells voltage clamped at −70 mV in TTX (500 nM), picrotoxin (100 μM) and APV (50 μM). mEPSCs were collected using pClamp 10 and analyzed using Mini60 Mini Analysis Program (Synaptosoft). Detection criteria were set at > 15 pA, < 3 ms rise-time, and < 3 ms decay-time for AMPAR mEPSCs. For preincubation experiments, compounds were bath applied at least 20 minutes before insulin application unless otherwise specified in the text. In some experiment, compounds were applied intracellularly via the patch pipette.

Surgical Procedures - Mice

Animals (C57BL/6J males; 25 to 27 g at start of experiment) were housed individually on a 12-hour light/dark cycle (lights on at 6 am) at a constant temperature (21°C). Mice were given access to standard laboratory rodent chow and water *ad libitum* prior to and for 14 days following surgery. Before bilateral intracranial cannulae implantation, animals were anesthetized with an intraperitoneal injection of 3:1 ketamine:xylazine and placed in a stereotaxic frame (Kopf; Tujunga, CA). 26 gauge bilateral guide cannulae (Plastics One, Roanoke, VA) were lowered into the VTA (AP, −3.2 mm; ML, ±0.5 mm; DV, −4.6 mm). Cannulae were anchored to the skull surface with dental cement and occluded with metal obturators of the same length. Mice were treated post-surgically with ketoprofen (5 mg/kg, s.c.). Weights were monitored daily to ensure appropriate weight gain. Mice recovered for 14 days.

Cocaine-induced locomotor activity

Mice were cannulated as above. Mice were given one hour access to SHF or RF and then an intra-VTA injection of saline. 10 min after the microinjection, mice were given cocaine (10 mg/kg, i.p.) and then placed in an open field chamber for 15 min.

Food Anticipatory Activity Experiment

After recovery from surgery mice were given standard mouse chow (6 % fat, 44 % carbohydrate, Harlan Laboratories diet 2018) and entrained to consume their daily caloric

needs within 4 hours per day (12–4pm, PST) in a novel entrainment cage with kitty litter bedding. The amount of chow consumed was weighed hourly and the animals were weighed daily after the 4 hour entrainment period. Mice were entrained for 19 days prior to VTA microinjections. Over the course of the experiment, mice maintained their weight between 27–30g. Microinfusions were conducted using a 33 gauge cannula that protruded 0.2 mm below the base of the cannulae to a final DV coordinate of 4.8 mm. Insulin (5 mU in 10 % DMSO) or vehicle (10 % DMSO in saline) was infused bilaterally into the VTA (0.2 μl at 0.1 μl/min). Microinjectors were left in place for 2 min and then mice were placed in home cages for 10 min prior to access to feeding in the entrainment cages. On test days, mice received either vehicle or insulin. The order of drug delivery was reversed on subsequent test days in an order-counterbalanced crossover experimental design.

After microinfusions, mice were placed in their entrainment cage with a transparent plexiglass barrier with 4 small holes 3 cm from the base of the barrier separating the mice from their food. Activity was digitally recorded and analyzed posthoc. After 15 min, the barrier was lifted and mice had access to their food. Several behavioral activities were recorded from a single session. Crossovers were defined as the number of times the mouse crossed a center line in the barriered section of the cage. Rearing was defined as the amount of time the animal reared on hind legs. Digging was defined as the amount of time the mouse spent digging bedding at the barrier or elsewhere in the cage. Placements were determined post hoc and are presented in Supplemental Figure 3. To measure basal locomotor activity, mice were microinjected with insulin (5 mU) or vehicle 10 min prior to placement in an open field chamber. Locomotor activity was recorded in 5 min bins and monitored for 30 min. Two days later, the order of drug delivery was reversed on a subsequent test day in an order-counterbalanced crossover experimental design.

Progressive Ratio Experiment

C57BL/6J males (25 to 30 g) were used for behavioral experiments in agreement with the Swiss Federal Act on Animal Protection and the Swiss Animal Protection Ordinance and were approved by the district veterinary office. Animals were housed individually under 12-hour reversed dark/light cycle (lights on at 8 pm) at a constant temperature (21°C) and had ad libitum access to laboratory chow and tap water. Mice were cannulated as above. Two weeks after surgery, mice were trained in fixed ratio 1 (FR1) sessions in standard operant chambers (17.5x15x18cm, Med Associates, St Albans, VT, USA) with two nose poke ports, each associated with a cue light and a central spout for liquid delivery equipped with an infrared head entry detector. Each active nose poke resulted in the delivery of a 10 μL 2.5% sucrose or sweetened condensed milk, in addition to a 3-sec cue light illumination over the active port. Liquid rewards remained available for 3 sec once access to the liquid dipper was detected with head entry detectors. During this period, additional nosepoke entries were still recorded but had no further consequence. Mice received 25 additional days of 30 min daily sessions until stable nose poking (minimum 20 active nose pokes with less than 20% variance) was reached. Then mice were switched to 2 consecutive 90 min sessions using a progressive ratio (PR) schedule of reinforcement. Under this schedule, the number of responses required to obtain each successive reinforcer was determined by the equation (Richardson and Roberts, 1996), Response ratio = $[5e^{(\text{injection number} \times 0.2)}]-5$ to produce the

following sequence of required lever presses: 1, 2, 4, 6, 9, 12, 15, 25, 32, 40, 50, 62, etc. The maximal number of presses emitted to attain the final ratio was defined as the breakpoint[43]. Bilateral infusions of insulin (0.065 mU (2 μM) or 3.25 mU (100 μM)), 0.2μl at 1 μl/min) or vehicle (0.2μl at 1 μl/min) were delivered 20 min prior to the PR session. The order of drug delivery was reversed on subsequent test days in order-counterbalanced crossover experimental design. Placements were determined post hoc and are presented in Supplemental Figure 3.

Conditioned Place Preference Experiment

Male Sprague-Dawley rats (Charles River, Montreal, Canada) weighing 200–220 g upon arrival, were pair-housed (light on 7:00–19:00 h). Rats had *ad libitum* access to water and food. All experiments followed the principles of laboratory animal care and were conducted in accordance with the standards of the Canadian Council on Animal Care and the Guidelines for the Care and Use of Mammals in Neuroscience and Behavioral Research (National Research Council 2003). All the experiments were approved by the Committee on Animal Care, University of British Columbia. One week following their arrival, rats were anaesthetized with Isoflurane (Oxygen flow rate: 2L/min; Isoflurane: Induction: 4%; Maintenance: 1.5–2.5%; Baxter corporation, Canada). Bilateral 23 gauge stainless steel guide cannulae were implanted 1.5 mm above the Ventral Tegmental Area (VTA). The coordinates based on the rat brain atlas (Paxinos and Watson, 1997) were the following: Anteroposterior: −5.6 mm; Mediolateral: ±0.5; Dorsoventral:−6.5 mm. The cannula was then secured to the skull using the dental cement anchored with 4 screws. A 30 gauge stainless steel dummy cannula was inserted into the guide cannula to prevent particles from entering the cannula. After 1 week of recovery, the animals began the behavioral experiment. Each CPP apparatus was constructed from acrylic panels and contained two larger rectangular compartments (47.2 cm × 24.6 cm × 31.5 cm) separated by guillotine doors from a white smaller neutral zone with a smooth Plexiglass floor (21 cm × 16 cm × 31.5 cm). The two large compartments differed with respect to contextual cues; one contained four black and white stripe walls with a wire mesh floor and the other one had gray walls with a Plexiglass bar floor. A digital camera placed above each apparatus transmitted data to a computer for analysis with appropriate software (Ethovision, Noldus) providing an accurate measure of time spent in each compartment. A pre-conditioning test ensured that the animals did not have a preference for a compartment. The animals were placed in the middle compartment and had access to the entire apparatus for 15 min. The time spent in each compartment was recorded. Rats were then assigned in a counterbalanced manner to different treatment groups, and trained according to an unbiased protocol. Following the pre-conditioning session, rats were placed in one compartment with 40 Froot Loops in a food tray and on alternate days, they were confined in the other compartment with an empty food tray. Each conditioning session lasted 25 min for 8 days of conditioning. On the test day, animals received either intra-VTA insulin (0.005 mU (63 nM) or 0.065 mU (2 μM)) or vehicle (ACSF; 0.5 μl/hemisphere at 0.25 μl/min) 5 min prior to being placed in the CPP apparatus for 15 min. Time spent in each compartment in the absence of food was recorded. Placements were determined post hoc and are presented in supplemental figure 3.

Plasma insulin measurements

Blood samples were taken from ad-lib fed P19-30 C57BL/6J mice immediately after 1hour access to regular chow food (RF) or sweetened high fat food (SHF) or 1h after SHF. Samples were centrifuged at 14,000 rpm for 10 min at 4°C to separate plasma. The concentration of plasma insulin was determined using an enzyme-linked immunosorbent assay (ELISA) according to instructions of the Mouse Ultrasensitive Insulin ELISA kit from Alpco (Salem, NH).

Data Analysis

All values are expressed as mean ± SEM. Statistical significance was assessed using two-tailed Student's t tests. For electrophysiology experiments, "n" refers to the number of cells recorded from. For each experiment several cells from 3 or more mice were used. A one-way ANOVA followed by a post hoc test was used for multiple group comparisons. Statistics on cumulative probability curves were performed using a Kolmogorov–Smirnov test. Prism 5 software (GraphPad Software, Inc., La Jolla, CA) was used to perform statistical analysis. Figures were generated using Illustrator CS2 software (Adobe Systems Incorporated). The levels of significance are indicated as follows: *** $p < 0.001$, ** $p < 0.01$, * $p < 0.05$.

Drugs

All reagents were supplied by Tocris Bioscience, except for insulin (Zn^{2+}-free), orlistat and picrotoxin which were supplied by Sigma-Aldrich, WIN 55212-2 by Cayman Chemical, S15 by CPC Scientific Inc. and HNMPA by Calbiochem. S961 was kindly provided by L. Schaffer as a gift (Novo Nordisk A/S, Maaloev, Denmark).

Supplementary Material

Refer to Web version on PubMed Central for supplementary material.

Acknowledgments

The authors would like to thank Ms. Katie Lee for performing the insulin measurements, and Drs. Kurt Haas, Brian MacVicar and Yu Tian Wang for their helpful suggestions on the manuscript. This research was supported by a CIHR operating grant and a CIHR new investigator award to S.L.B. G.L was supported by a Swiss National Science Foundation postdoctoral fellowship.

References

1. Gerozissis K. Brain insulin, energy and glucose homeostasis; genes, environment and metabolic pathologies. Eur J Pharmacol. 2008; 585:38–49. [PubMed: 18407262]
2. Palmiter RD. Is dopamine a physiologically relevant mediator of feeding behavior? Trends Neurosci. 2007; 30:375–381. [PubMed: 17604133]
3. Bonci A, Malenka RC. Properties and plasticity of excitatory synapses on dopaminergic and GABAergic cells in the ventral tegmental area. J Neurosci. 1999; 19:3723–3730. [PubMed: 10234004]
4. Overton PG, Richards CD, Berry MS, Clark D. Long-term potentiation at excitatory amino acid synapses on midbrain dopamine neurons. Neuroreport. 1999; 10:221–226. [PubMed: 10203312]
5. Borgland SL, et al. Orexin A/hypocretin-1 selectively promotes motivation for positive reinforcers. J Neurosci. 2009; 29:11215–11225. [PubMed: 19741128]

6. Borgland SL, Taha SA, Sarti F, Fields HL, Bonci A. Orexin A in the VTA is critical for the induction of synaptic plasticity and behavioral sensitization to cocaine. Neuron. 2006; 49:589–601. [PubMed: 16476667]
7. Abizaid A, et al. Ghrelin modulates the activity and synaptic input organization of midbrain dopamine neurons while promoting appetite. J Clin Invest. 2006; 116:3229–3239. [PubMed: 17060947]
8. Thompson JL, Borgland SL. A role for hypocretin/orexin in motivation. Behav Brain Res. 2011; 217:446–453. [PubMed: 20920531]
9. Blum ID, et al. Reduced anticipatory locomotor responses to scheduled meals in ghrelin receptor deficient mice. Neuroscience. 2009; 164:351–359. [PubMed: 19666088]
10. Baskin DG, et al. Insulin and leptin: dual adiposity signals to the brain for the regulation of food intake and body weight. Brain Res. 1999; 848:114–123. [PubMed: 10612703]
11. Woods SC, Seeley RJ, Baskin DG, Schwartz MW. Insulin and the blood-brain barrier. Curr Pharm Des. 2003; 9:795–800. [PubMed: 12678878]
12. Woods SC, D'Alessio DA. Central control of body weight and appetite. J Clin Endocrinol Metab. 2008; 93:S37–50. [PubMed: 18987269]
13. Mielke JG, et al. A biochemical and functional characterization of diet-induced brain insulin resistance. J Neurochem. 2005; 93:1568–1578. [PubMed: 15935073]
14. Hommel JD, et al. Leptin receptor signaling in midbrain dopamine neurons regulates feeding. Neuron. 2006; 51:801–810. [PubMed: 16982424]
15. Fulton S, Pissios P, Manchon RP, Stiles L, Frank L, Pothos EN, Maratos-Flier E, Flier JS. Leptin regulation of the mesoaccumbens dopamine pathway. Neuron. 2006; 51:811–822. [PubMed: 16982425]
16. Figlewicz DP, Evans SB, Murphy J, Hoen M, Baskin DG. Expression of receptors for insulin and leptin in the ventral tegmental area/substantia nigra (VTA/SN) of the rat. Brain Res. 2003; 964:107–115. [PubMed: 12573518]
17. Figlewicz DP, Bennett JL, Naleid AM, Davis C, Grimm JW. Intraventricular insulin and leptin decrease sucrose self-administration in rats. Physiol Behav. 2006; 89:611–616. [PubMed: 17045623]
18. Figlewicz DP, et al. Intraventricular insulin and leptin reverse place preference conditioned with high-fat diet in rats. Behav Neurosci. 2004; 118:479–487. [PubMed: 15174925]
19. Sipols AJ, Bayer J, Bennett R, Figlewicz DP. Intraventricular insulin decreases kappa opioid-mediated sucrose intake in rats. Peptides. 2002; 23:2181–2187. [PubMed: 12535697]
20. Figlewicz DP, Bennett JL, Aliakbari S, Zavosh A, Sipols AJ. Insulin acts at different CNS sites to decrease acute sucrose intake and sucrose self-administration in rats. Am J Physiol Regul Integr Comp Physiol. 2008; 295:R388–394. [PubMed: 18525010]
21. Mebel DM, Wong JC, Dong YJ, Borgland SL. Insulin in the ventral tegmental area reduces hedonic feeding and suppresses dopamine concentration via increased reuptake. Eur J Neurosci. 2012; 36:2336–3346. [PubMed: 22712725]
22. Bruijnzeel AW, Corrie LW, Rogers JA, Yamada H. Effects of insulin and leptin in the ventral tegmental area and arcuate hypothalamic nucleus on food intake and brain reward function in female rats. Behav Brain Res. 2011; 219:254–264. [PubMed: 21255613]
23. Overton PG, Clark D. Burst firing in midbrain dopamine neurons. Brain Res Brain Res Rev. 1997; 25:312–334. [PubMed: 9495561]
24. Watabe-Uchida M, Zhu L, Ogawa SK, Vamanrao A, Uchida N. Whole-brain mapping of direct inputs to midbrain dopamine neurons. Neuron. 2012; 74:858–73. [PubMed: 22681690]
25. Wang YT, Linden DJ. Expression of cerebellar long-term depression requires postsynaptic clathrin-mediated endocytosis. Neuron. 2000; 25:635–647. [PubMed: 10774731]
26. Man HY, et al. Regulation of AMPA receptor-mediated synaptic transmission by clathrin-dependent receptor internalization. Neuron. 2000; 25:649–662. [PubMed: 10774732]
27. Baltensperger K, et al. Catalysis of serine and tyrosine autophosphorylation by the human insulin receptor. Proc Natl Acad Sci U S A. 1992; 89:7885–7889. [PubMed: 1381504]

28. Schaffer L, et al. A novel high-affinity peptide antagonist to the insulin receptor. Biochem Biophys Res Commun. 2008; 376:380–383. [PubMed: 18782558]
29. Vigneri R, Squatrito S, Sciacca L. Insulin and its analogs: actions via insulin and IGF receptors. Acta diabetologica. 2010; 47:271–278. [PubMed: 20730455]
30. Asnaghi L, Bruno P, Priulla M, Nicolin A. mTOR: a protein kinase switching between life and death. Pharmacol Res. 2004; 50:545–549. [PubMed: 15501691]
31. Mameli M, Balland B, Lujan R, Luscher C. Rapid synthesis and synaptic insertion of GluR2 for mGluR-LTD in the ventral tegmental area. Science. 2007; 317:530–533. [PubMed: 17656725]
32. Malinow R, Malenka RC. AMPA receptor trafficking and synaptic plasticity. Annu Rev Neurosci. 2002; 25:103–126. [PubMed: 12052905]
33. Brebner K, et al. Nucleus accumbens long-term depression and the expression of behavioral sensitization. Science. 2005; 310:1340–1343. [PubMed: 16311338]
34. Lee CC, Huang CC, Wu MY, Hsu KS. Insulin stimulates postsynaptic density-95 protein translation via the phosphoinositide 3-kinase-Akt-mammalian target of rapamycin signaling pathway. J Biol Chem. 2005; 280:18543–18550. [PubMed: 15755733]
35. Luscher C, et al. Role of AMPA receptor cycling in synaptic transmission and plasticity. Neuron. 1999; 24:649–658. [PubMed: 10595516]
36. Kauer JA, Malenka RC. Synaptic plasticity and addiction. Nat Rev Neurosci. 2007; 8:844–858. [PubMed: 17948030]
37. Katz B. Quantal mechanism of neural transmitter release. Science. 1971; 173:123–126. [PubMed: 4325812]
38. Melis M, et al. Endocannabinoids mediate presynaptic inhibition of glutamatergic transmission in rat ventral tegmental area dopamine neurons through activation of CB1 receptors. J Neurosci. 2004; 24:53–62. [PubMed: 14715937]
39. Heifets BD, Castillo PE. Endocannabinoid signaling and long-term synaptic plasticity. Annual review of physiology. 2009; 71:283–306.
40. Bisogno T, et al. Brain regional distribution of endocannabinoids: implications for their biosynthesis and biological function. Biochem Biophys Res Commun. 1999; 256:377–380. [PubMed: 10079192]
41. Blum ID, Waddington-Lamont E, Rodrigues T, Abizaid A. Isolating neural correlates of the pacemaker for food anticipation. PLoS One. 2012; 7:e36117. [PubMed: 22558352]
42. Ahn S, Phillips AG. Dopaminergic correlates of sensory-specific satiety in the medial prefrontal cortex and nucleus accumbens of the rat. J Neurosci. 1999; 19:RC29. [PubMed: 10493774]
43. Richardson NR, Roberts DC. Progressive ratio schedules in drug self-administration studies in rats: a method to evaluate reinforcing efficacy. J Neurosci Methods. 1996; 66:1–11. [PubMed: 8794935]
44. Schoffelmeer AN, Drukarch B, De Vries TJ, Hogenboom F, Schetters D, Pattij T. Insulin modulates cocaine-sensitive monoamine transporter function and impulsive behavior. J Neurosci. 2011; 31:1284–1291. [PubMed: 21273413]
45. Sanchis-Segura C, Spanagel R. Behavioural assessment of drug reinforcement and addictive features in rodents: an overview. Addict Biol. 2006; 11:2–38. [PubMed: 16759333]
46. Pan B, Hillard CJ, Liu QS. Endocannabinoid signaling mediates cocaine-induced inhibitory synaptic plasticity in midbrain dopamine neurons. J Neurosci. 2008; 28:1385–1397. [PubMed: 18256258]
47. Henny P, Brown MT, Northrop A, Faunes M, Ungless MA, Magill PJ, Bolam JP. Structural correlates of heterogeneous in vivo activity of midbrain dopaminergic neurons. Nat Neurosci. 2012; 15:613–619. [PubMed: 22327472]
48. Grueter BA, Brasnjo G, Malenka RC. Postsynaptic TRPV1 triggers cell type-specific long-term depression in the nucleus accumbens. Nat Neurosci. 2010; 13:1519–1525. [PubMed: 21076424]
49. Gerdeman GL, Ronesi J, Lovinger DM. Postsynaptic endocannabinoid release is critical to long-term depression in the striatum. Nat Neurosci. 2002; 5:446–451. [PubMed: 11976704]

50. Ronesi J, Gerdeman GL, Lovinger DM. Disruption of endocannabinoid release and striatal long-term depression by postsynaptic blockade of endocannabinoid membrane transport. J Neurosci. 2004; 24:1673–1679. [PubMed: 14973237]
51. Yin HH, Davis MI, Ronesi JA, Lovinger DM. The role of protein synthesis in striatal long-term depression. J Neurosci. 2006; 26:11811–11820. [PubMed: 17108154]
52. Massa F, Mancini G, Schmidt H, Steindel F, Mackie K, Angioni C, Oliet SH, Geisslinger G, Lutz B. Alterations in the hippocampal endocannabinoid system in diet-induced obese mice. J Neurosci. 2010; 30:6273–6281. [PubMed: 20445053]
53. Lüscher C, Malenka RC. Drug-evoked synaptic plasticity in addiction: from molecular changes to circuit remodeling. Neuron. 2012; 69:650–663.
54. Duckworth WC, Bennett RG, Hammel FG. Insulin degradation: Progress and potential. Endocrine Rev. 1998; 19:608–624. [PubMed: 9793760]
55. Borgland SL, Taha SA, Sarti F, Fields HL, Bonci A. Orexin a in the VTA is critical for the induction of synaptic plasticity and behavioral sensitization to cocaine. Neuron. 2006; 49:589–601. [PubMed: 16476667]
56. Borgland SL, Storm E, Bonci A. Orexin B/hypocretin 2 increases glutamatergic transmission to ventral tegmental area neurons. Eur J Neurosci. 2008; 28:1545–1556. [PubMed: 18793323]
57. Abizaid A, Liu ZW, Andrews ZB, Shanabrough M, Borok E, Elsworth JD, et al. Ghrelin modulates the activity and synaptic input organization of midbrain dopamine neurons while promoting appetite. J Clin Invest. 2006; 116:3229–3239. [PubMed: 17060947]
58. Tsai HC, Zhang F, Adamantidis A, Stuber GD, Bonci A, de Lecea L, Deisseroth K. Phasic firing in dopaminergic neurons is sufficient for behavioral conditioning. Science. 2009; 324:1080–1084. [PubMed: 19389999]
59. Stuber GD, et al. Reward-predictive cues enhance excitatory synaptic strength onto midbrain dopamine neurons. Science. 2008; 321:1690–1692. [PubMed: 18802002]
60. Mebel DM, Wong JC, Dong YJ, Borgland SL. Insulin in the ventral tegmental area reduces hedonic feeding and suppresses dopamine concentration via increased reuptake. Eur J Neurosci. 2012; 36:2336–2346. [PubMed: 22712725]
62. Yoshizaki T, et al. Isolation and transplantation of dopaminergic neurons generated from mouse embryonic stem cells. Neuroscience Lett. 2004; 363:33–37.
63. Johnson SW, North RA. Two types of neurone in the rat ventral tegmental area and their synaptic inputs. J Physiol. 1992; 450:455–468. [PubMed: 1331427]
64. Lacey MG, Mercuri NB, North RA. Actions of cocaine on rat dopaminergic neurones in vitro. Br J Pharmacol. 1990; 99:731–735. [PubMed: 2361170]

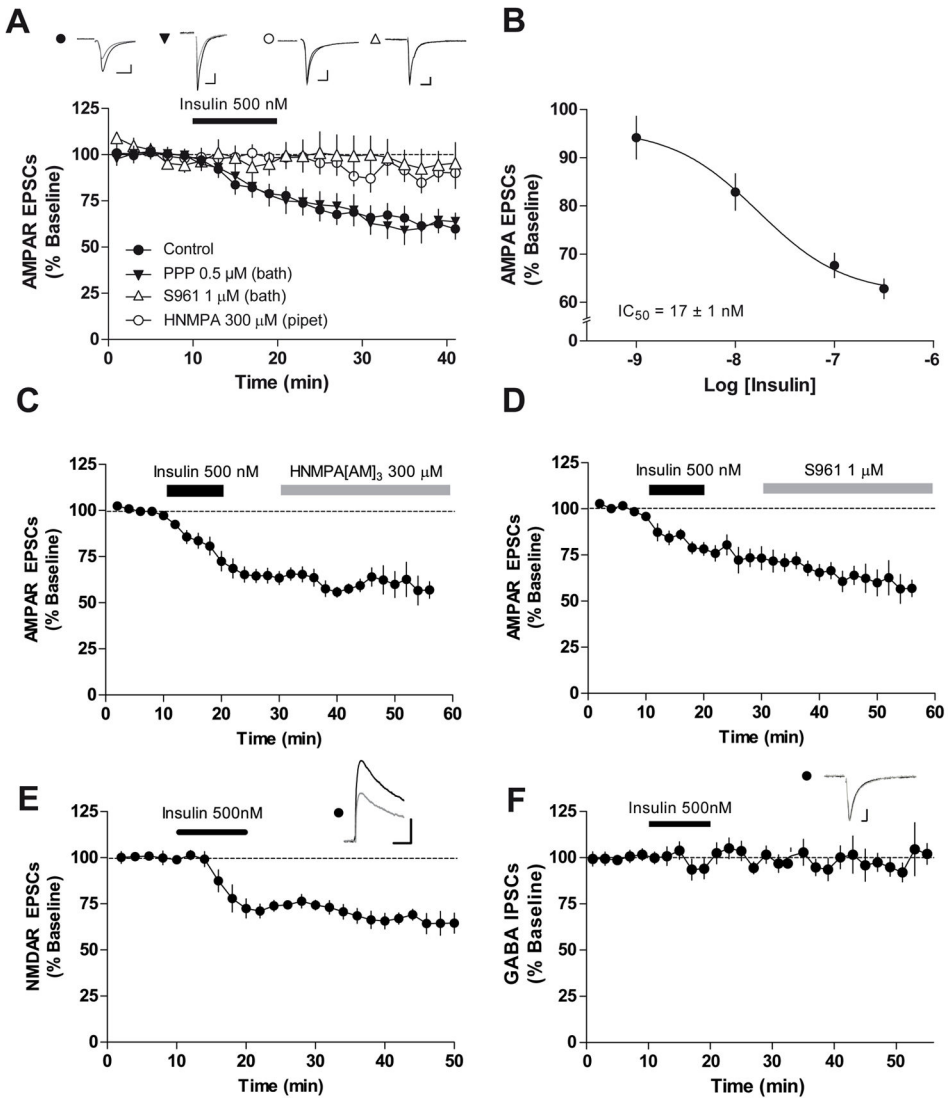

Figure 1. Insulin depresses AMPAR-mediated synaptic transmission onto VTA dopamine neurons

Evoked AMPAR EPSCs were recorded before during and after bath application of insulin (10 min). (**A**) Insulin depressed AMPAR EPSC amplitude in VTA dopamine neurons (filled circles, n = 9). Intracellular application of HNMPA (300 μM), an insulin receptor tyrosine kinase inhibitor (open circles, n = 7), or bath application of an insulin receptor antagonist (peptide S961) throughout the experiment (open triangles, n = 7, 1 μM) blocked insulin-induced depression of AMPAR synaptic transmission. The selective IGFR inhibitor picropodophyllotoxin (PPP; 0.5 μM), applied before during and after insulin application (500 nM, 10 min), blocked insulin-induced depression of AMPAR EPSCs (filled triangles, n = 8). Example recordings of AMPAR EPSCs at 5 (black) and 40 (grey) min are shown above of the time course. Scale bars, 10 ms and 50 pA. (**B**) A concentration-response curve of maximal insulin effect taken at 40 min for each concentration is fit with a sigmoidal curve. Insulin depressed AMPAR excitatory transmission onto VTA dopaminergic neurons in a dose-dependent manner (1, 10, 100 or 500 nM with n = 5, 6, 5 or 7, respectively). (**C**) Bath

application of cell permeable HNMPA[AM]3 (300 μM) did not reverse insulin-induced LTD (n = 6). (**D**) Insulin receptor antagonist (S961, 1 μM) did not reverse insulin-induced LTD (n = 6). (**E**) Evoked NMDAR EPSCs were recorded before during and after bath application of insulin (10 min). Bath application of insulin (500 nM, 10 min) depressed NMDAR EPSC amplitude in VTA dopamine neurons (filled circles, n = 9). Example recording of NMDAR EPSCs at 5 (black) and 40 (grey) min is shown above of the time course. Scale bars, 10 ms and 50 pA. (**F**) Bath application of insulin (500 nM, 10 min) did not depress $GABA_A$ IPSCs amplitude in VTA dopamine neurons (filled circles, n = 7). Traces of $GABA_A$ IPSCs overlaid at 5 (black) and 40 (grey) min are shown on top of the time course. Scale bars, 5 ms and 50 pA. Stimulus artifacts have been removed for clarity. Error bars represent s.e.m.

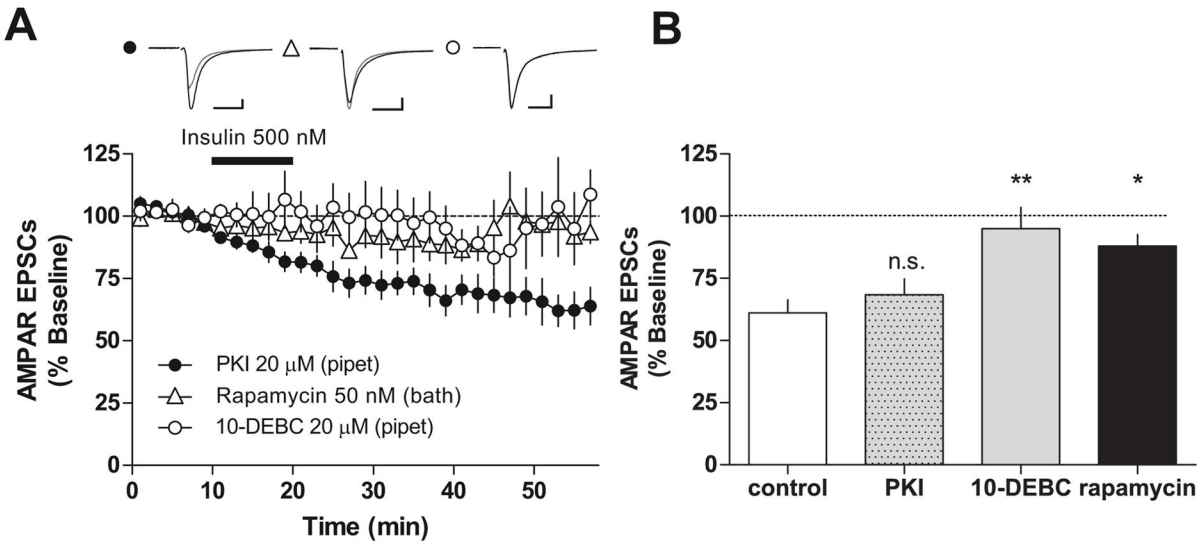

Figure 2. Insulin-induced LTD requires Akt and mTOR signaling

(**A**) Bath application of rapamycin (50 nM, open triangles, n = 7), an inhibitor of mTOR signaling, or intracellular application of 10-DEBC (20 μM), a selective inhibitor of Akt (open circles, n = 7), blocked insulin-induced LTD. Intracellular application of PKI (20 μM, filled circles, n = 7), a protein kinase A inhibitor, did not alter insulin-induced LTD. Example recordings of overlaid AMPAR EPSCs at 5 (black) and 40 (grey) min in the presence of rapamycin (open triangle), 10-DEBC (open circle) or PKI (filled circle) are shown on top of the time course. Scale bars, 5 ms and 50 pA. (**B**) A bar graph showing the averaged AMPAR EPSCs 20 min after insulin application for control (Insulin alone, open bars); in the presence of PKI (patterned bar), 10-DEBC (shaded bar) or rapamycin (filled bar). Using one-way ANOVA with a Dunnet's post hoc test comparing treatments to control, we found that 10-DEBC or Rapamycin treatments were significantly different from insulin treatment (** $p<0.01$, * $p<0.05$). Stimulus artifacts have been removed for clarity. Error bars represent s.e.m.

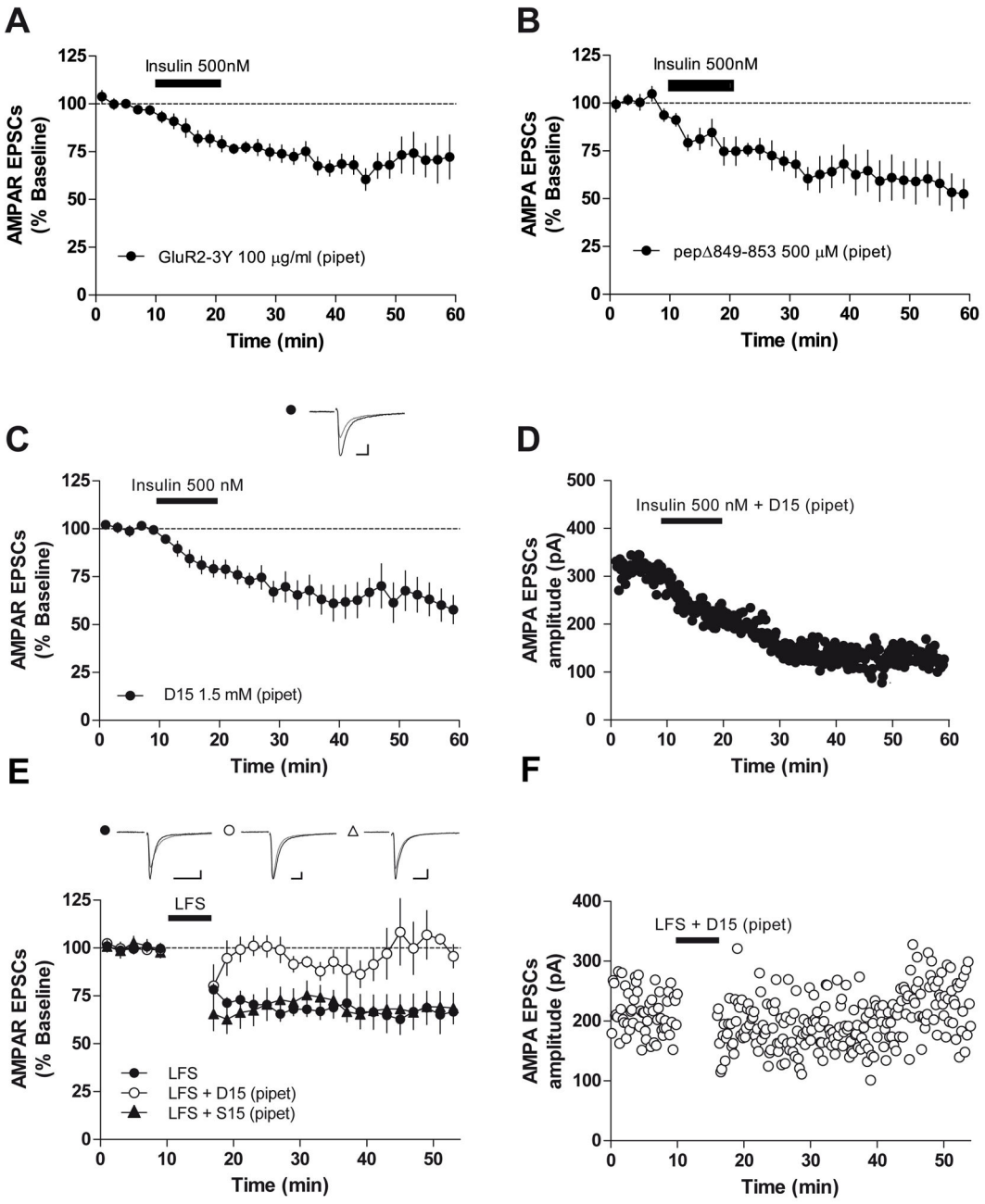

Figure 3. Insulin-induced LTD in the VTA does not require endocytosis of AMPARs

(**A**) Intracellular application of GluR2-3Y (100 µg/ml), an AMPAR endocytosis inhibitor that blocks the interaction AP2 with the GluA2 subunit, did not alter insulin-induced LTD of AMPARs (n = 8). (**B**) Intracellular application of pepΔ849-853 (500 µM) did not alter insulin-induced LTD (n = 4). (**C**) Intracellular application of D15 (1.5 mM), an endocytosis inhibitor that blocks the interaction of dynamin with amphiphysin, did not alter insulin-induced LTD of AMPARs (n = 7). (**D**) Example time course of AMPAR EPSCs amplitude in a single dopamine neuron in the presence of D15. (**E**) A low-frequency stimulation protocol (LFS, −40 mV, 6 min, 1 Hz stimulation) induced LTD in VTA dopamine neurons (filled

circles, n = 8). Intracellular application of D15 blocked LFS-LTD (open circles, n = 6). S15 (1.5 mM), a scrambled version of the D15 peptide, did not affect LFS-LTD when applied intracellularly (filled triangles, n = 8). (**F**) Example time course of AMPAR EPSCs amplitude recorded before and after LFS in the presence of D15. Traces of AMPAR EPSCs overlaid at 5 (black) and 40 (grey) min are shown on top of the time course. Scale bars, 5 ms and 50 pA. Stimulus artifacts have been removed for clarity. Error bars represent s.e.m.

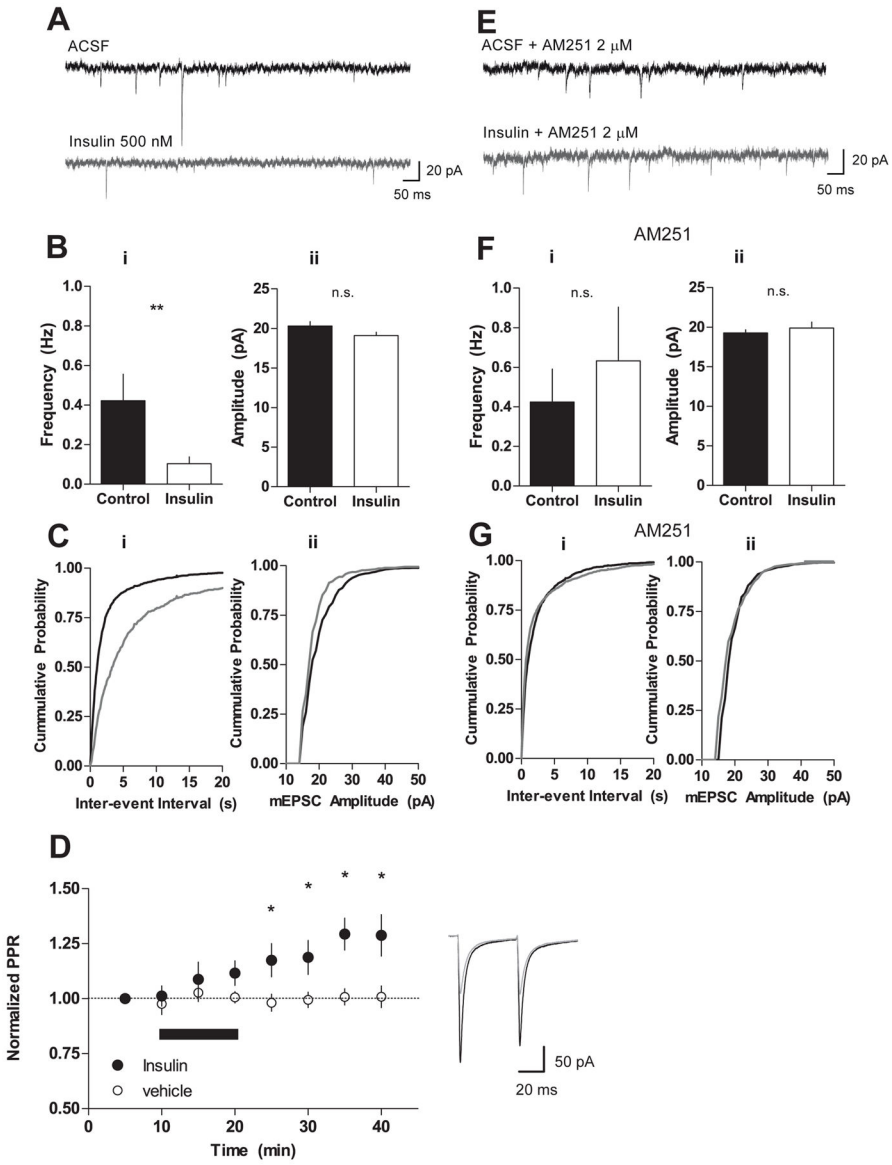

Figure 4. Insulin-induced LTD occurs presynaptically and requires CB1R activation

(**A**) Example recordings of AMPAR miniature EPSCs (mEPSCs) of VTA dopamine neurons 20 to 30 min after 10 min preincubation with ACSF (left) or ACSF + insulin (500 nM, right). Scale bars, 50 ms and 20 pA. (**B**i) Frequency of mEPSCs events was significantly decreased after insulin treatment (open bars, n = 11) compared to control (filled bars, n = 11, $p < 0.01$). (**Bii**) AMPAR mEPSCs amplitude was not significantly different after insulin treatment (open bars, n = 11) compared to slices treated with ACSF (filled bars, n = 10, $p > 0.05$). (**C**) Cumulative probability plots for inter-event interval (i) or mEPSCs amplitude (ii) measured from VTA slices 20 to 30 min after 10 min preincubation with ACSF (black line) or ACSF + insulin (500 nM, grey line) in example VTA neurons. (**D**) A time course demonstrating that a paired-pulse protocol using a 50-ms inter-stimulus interval showed facilitation after application of insulin (500 nM; filled circles; n = 6). The paired pulse ratio (PPR) was not significantly different with application of vehicle (open circles; n = 4). Right

panel, An example trace of a neuron recorded before (black) and 20 min (grey) after a 10-min insulin application. Stimulus artifact has been removed for clarity.
(**E**) Example recordings of AMPAR mEPSCs of VTA dopamine neurons 20 to 30 min after 10 min preincubation with ACSF (left) or ACSF + insulin (500 nM, right) in the presence of AM251 (2 μM). (**Fi**) In the presence of AM251, mEPSCs frequency after insulin treatment (open bars, n = 12) was not significantly different from controls (filled bars, n = 11, $p > 0.05$). (**Fii**) In slices preincubated with AM251, AMPAR mEPSCs amplitude was not significantly different after insulin treatment (open bars, n = 12) compared to control (filled bars, n = 11, $p > 0.05$). (**G**) Cumulative probability plots for inter-event interval (i) or mEPSCs amplitude (ii) measured from VTA slices 20 to 30 min after 10 min preincubation with ACSF (black line) or ACSF + insulin (500 nM, grey line) in presence of AM251 in example VTA neurons. A significant right-shift in the cumulative probability of mEPSC frequency was detected in insulin-treated slices as compared to control slices ($P<0.001$, Kolmogorov-Smirnov test). Bars represent mean ± s.e.m.

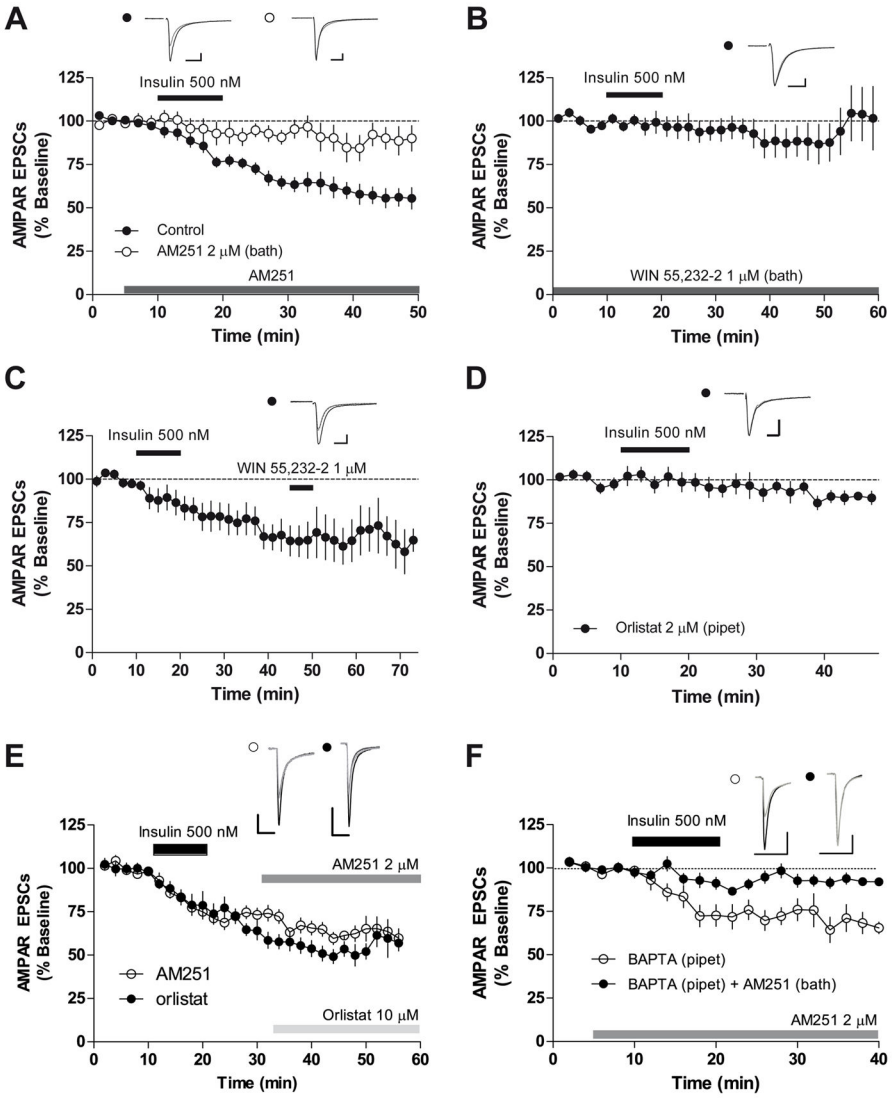

Figure 5. Insulin-induced LTD is mediated by endocannabinoid retrograde signaling

(**A**) Bath application of AM251 (2 μM) prior to insulin blocked insulin-induced LTD (open circles, n = 9) compared to insulin-induced LTD in the absence of AM251 (control, filled circles, n = 7). Inset, example traces of AMPAR EPSCs at 5 (black) and 40 (grey) min in the presence (open circle) or absence (filled circle) of AM251. Scale bars, 5 ms and 50 pA. (**B**) In slices preincubated with WIN (1 μM), insulin did not suppress AMPAR EPSCs (n = 7). Inset, example traces of AMPAR EPSCs at 5 and 40 min. Scale bars, 5 ms and 50 pA. (**C**) WIN (1 μM) was bath applied 25 min after a 10 min application of insulin (500 nM). WIN did not further alter insulin-induced LTD (n = 7). Inset, example traces of AMPAR EPSCs at 5 (black), 40 (grey) and 55 (hatched) min. Scale bars, 5 ms and 50 pA. (**D**) Intracellular application of orlistat (2 μM) abolished insulin-induced LTD (n = 6). Inset, example traces of AMPAR EPSCs at 5 (black) and 40 (grey) min. Scale bars, 5 ms and 50 pA. (**E**) Bath application of AM251 (2 μM; open circles; n = 7) or orlistat (10 μM; filled circles; n = 6) did not further alter insulin-induced LTD. Insets, example traces of AMPAR EPSCs at 5 (black), 30 (dark grey) and 50 (light grey) min. Scale bars, 10 ms and 50 pA. (**F**) Bath application of

insulin (500 nM) inhibited AMPAR EPSCs in the presence of intracellular BAPTA (10 mM; open circles) (n=9). Preincubation with AM251 (2 μM; filled circles) blocked insulin-induced LTD in the presence of intracellular BAPTA (10 mM) (n=9). Inset, example traces of AMPAR EPSCs at 5 (black) and 35 (grey) min in the presence of intracellular BAPTA (open circle) or BAPTA with AM251 (filled circle). Scale bars, 10 ms and 100 pA. Stimulus artifacts have been removed for clarity. Error bars represent s.e.m

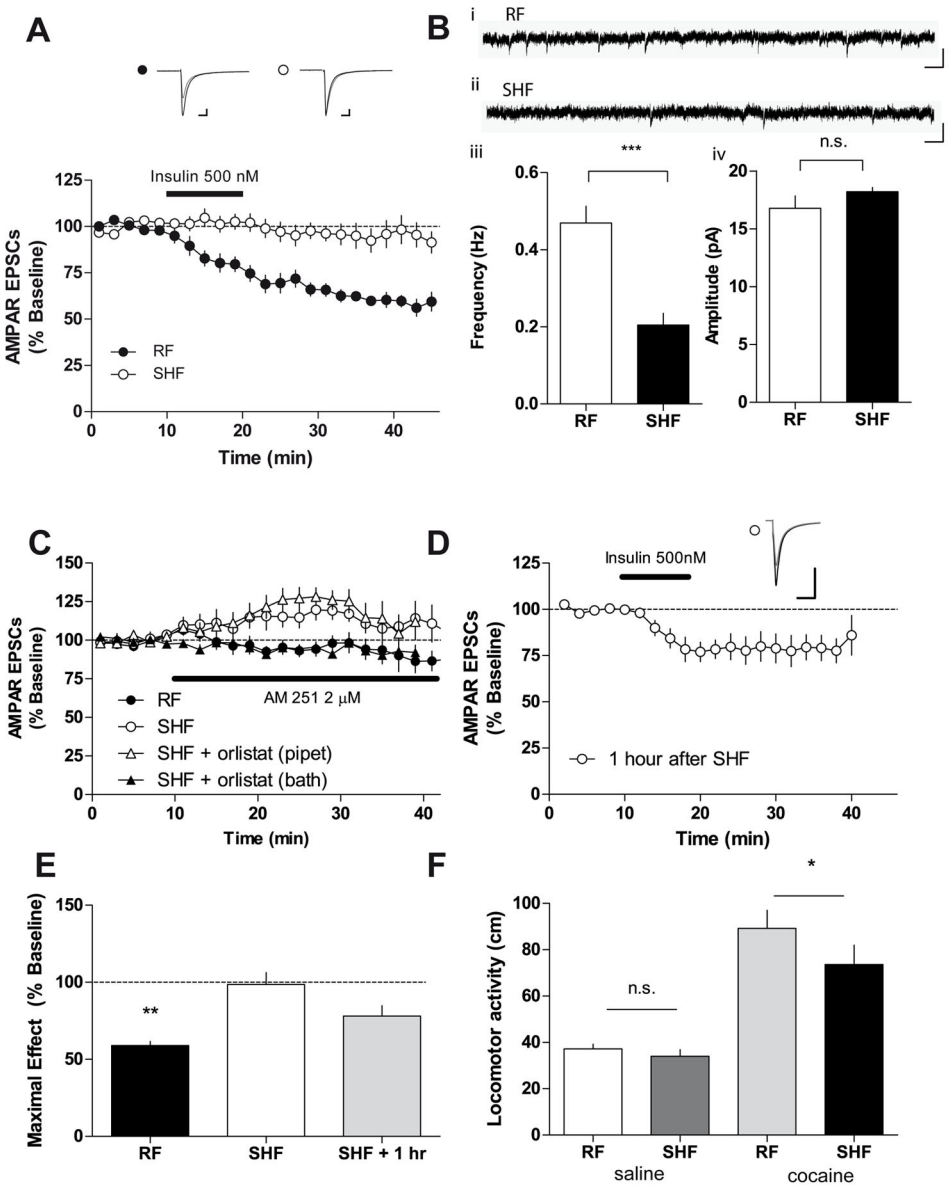

Figure 6. A sweetened high fat meal increases endocannabinoid tone and occludes insulin-induced LTD onto VTA dopamine neurons

(**A**) Bath application of insulin (500 nM, 10 min) did not depress AMPAR EPSCs amplitude in VTA dopamine neurons from animals fed with sweetened high-fat (SHF) food (1h access before sacrifice) in comparison with control animals fed with regular food (RF) chow (open circles, n = 11 and filled circles, n = 9, respectively). Example recording of AMPAR EPSCs at 5 (black) and 40 (grey) min is shown above of the time course. Scale bars, 5 ms and 50 pA. (**B**) (**i**) Example recordings of AMPAR mEPSCs of VTA dopamine neurons from non-food restricted mice given one hour access to RF (**ii**) or one hour access to SHF. Scale bars, 50 ms and 20 pA. (**iii**) Frequency of mEPSCs events was significantly decreased in mice fed SHF (filled bars, n = 11) compared to RF (open bars, n = 6, $p < 0.01$). (**iv**) AMPAR mEPSCs amplitude was not significantly different in mice fed RF (open bars, n = 11) compared to

mice fed SHF (filled bars, n = 6, $p > 0.05$). (**C**) Bath application of AM251 (2 μM) increased AMPAR EPSCs amplitude in VTA dopamine neurons from SHF-fed mice (open circles, n = 6), but not RF-fed mice (filled circles, n = 9). Intracellular orlistat (2 μM) did not alter AM251-induced increase in AMPAR EPSCs in SHF-fed mice (open triangles, n = 9). Bath application of orlistat (10 μM) inhibited the AM251-mediated increase in AMPAR EPSCs (filled triangles, n = 8). (**D**) Insulin-induced LTD was partially restored in VTA slices cut 1 hour after a SHF meal (n = 6). Inset, example traces of AMPAR EPSCs at 5 (black) and 40 (grey) min. Scale bars, 10 ms and 100 pA (**E**) Maximal effect of insulin-induced LTD in VTA slices cut immediately after mice were fed RF (open bars, n = 11) or SHF (filled bars, n = 9) or slices cut 1 hour after mice were fed SHF (grey bars; n = 6). (**F**) Cocaine-induced locomotor activity was significantly decreased in mice given 1 hour access to SHF (filled bar) compared to RF (light shaded) (n = 9, $p < 0.05$). Basal locomotor activity was not significantly different between SHF (open bar) and RF (dark shaded bar) groups (n = 6, $p > 0.05$). Stimulus artifacts have been removed for clarity. Bars represent means ± s.e.m.

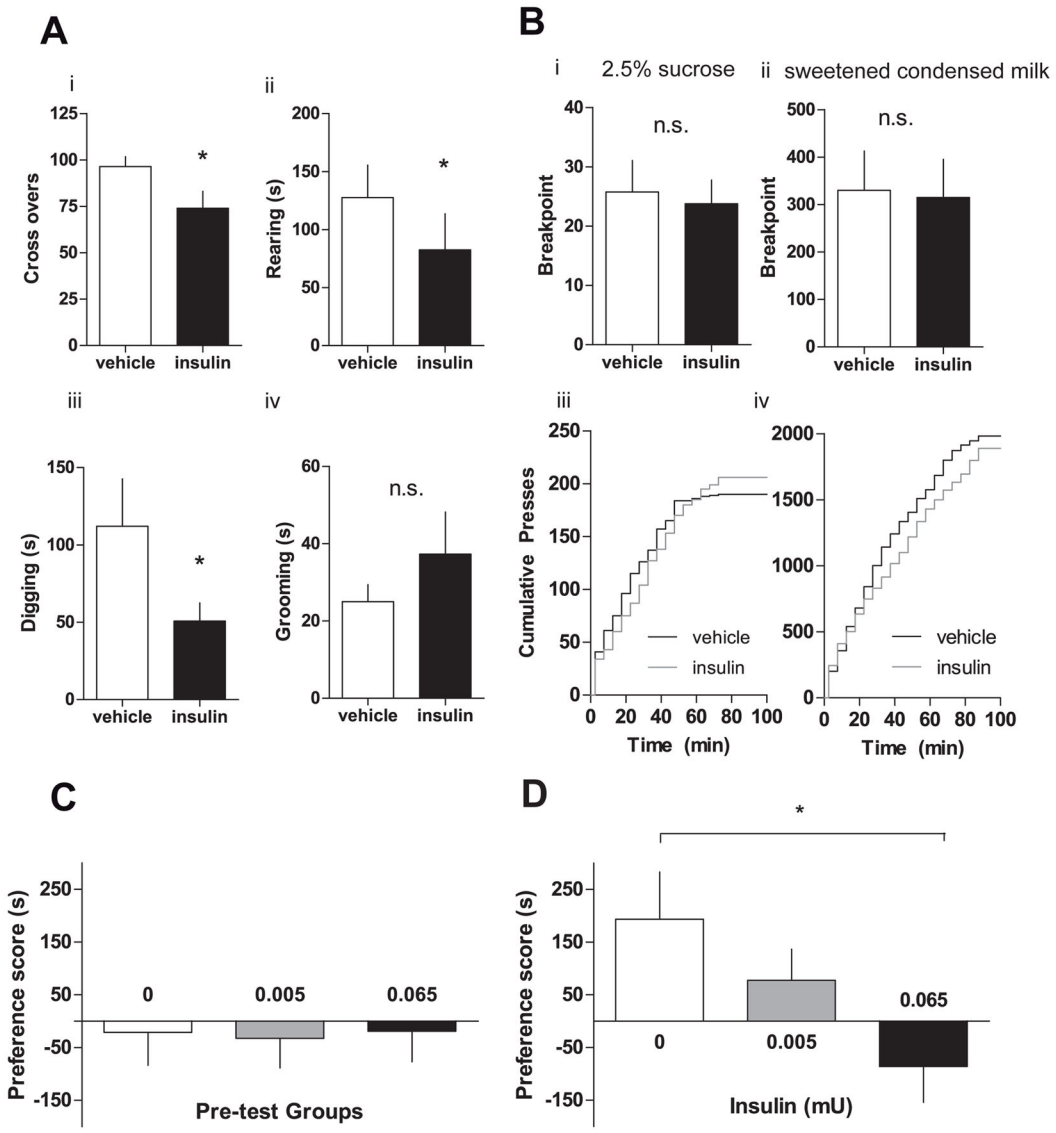

Figure 7. Insulin in the VTA decreases food anticipatory activity and conditioned place preference, but not effort

(A) Mice were entrained to eat their daily caloric needs 4 hours per day. On test days mice were microinjected with insulin (5 mU) or vehicle into the VTA 10 min prior to placing them in the entrainment cage with a plexiglass barrier separating the mice from the food. Insulin-treated mice (n = 7; filled bars) had significantly less food anticipatory activity measured by (**i**) cage cross overs, (**ii**) time spent rearing, and (**iii**) time spend digging than vehicle-treated mice (n = 7; open bars; $p < 0.05$). In contrast, (**iv**) grooming was not significantly different between insulin-treated and saline-treated mice (n = 7, $p > 0.05$). (**B**) Non-food restricted mice were trained to lever press for food under a progressive ratio schedule. Breakpoint was defined as the total number of lever presses required to receive the final reinforcer. (**i**) Breakpoint for 2.5% sucrose solution was not significantly different between mice receiving intra-VTA insulin (0.065 mU (2 μM)) or vehicle (n = 9; $p > 0.05$). (**ii**) Breakpoint for sweetened condensed milk was not significantly different between mice

receiving intra-VTA insulin (3.25 mU (100 μM)) or vehicle (n = 6; $p > 0.05$). (**iii**) Cumulative presses for 2.5% sucrose were not significantly different between mice receiving intra-VTA insulin (grey line) or vehicle (black line) ($p > 0.05$, Kolmogorov-Smirnov test). (**iv**) Cumulative presses for SCM were not significantly different between mice receiving intra-VTA insulin (grey line) or vehicle (black line) ($p > 0.05$, Kolmogorov-Smirnov test). (**C**) Non-food restricted rats were trained to associate one compartment with a palatable food (Froot Loops) in a CPP apparatus. Pre-test day training did not reveal a significant difference in preference score between groups ($p > 0.05$). (**D**) On the test day, rats were microinjected with insulin (0.005 mU (62 nM), 0.065 mU (2 μM)) or vehicle and placed in the neutral compartment of the CPP boxes. Preference scores were calculated by subtracting the time spent in the food-paired chamber from the time spent in the un-paired chamber. Intra-VTA insulin significantly reduced preference scores compared (n = 9; $p < 0.05$). Scores present group means ± s.e.m.